Arch. Metall. Mater., Vol. 61 (2016), No 4, p. 1999–2008

DOI: 10.1515/amm-2016-0323

M. RÓŻAŃSKI*, M. MORAWIEC**,#, A. GRAJCAR**, S. STANO*

MODIFIED TWIN-SPOT LASER WELDING OF COMPLEX PHASE STEEL

The work addresses modified methods of twin-spot laser welding of complex phase steel sheets and investigates the effects of laser beam distribution on the macrostructure, microstructure and hardness. The research-related results were obtained for the beam power distributions of 50%-50%, 60%-40% and 70%-30%. Test joints were made using a Yb:YAG disc laser with a maximum power of 12 kW and a welding head by means of which it was possible to focus a laser beam on two spots. It was found that the change in the laser beam distribution affects geometrical features of the joint. The application of the second beam of lower power enables obtaining tempering-like effects, which finally lead to the beneficial hardness reduction both in the fusion zone and in heat-affected zone. The identification of various microstructural constituents in different zones of the joint was performed using light microscopic micrographs and scanning electron images.

Keywords: laser welding, complex phase steel, metallurgical weldability, fine-grained microstructure, twin-spot welding

1. Introduction

The constant development of car body structures as well as growing demands related to passive safety and environmental friendliness make the steel industry intensively search for new grades of high strength steels [1-7]. Particularly intensively tested steels are referred to as Advanced High Strength Steels (AHHS), including DP and CP steels as well as steels demonstrating the effect of TRIP (TRansformation Induced Plasticity). A new generation of AHSS include high- and medium-manganese steels still undergoing various world-wide laboratory tests [8, 9].

Because of complicated shapes of car body elements, technologies predominantly used when joining the above-mentioned steels include laser welding and spot resistance welding [10]. An advantage of laser welding is low linear energy, if compared to that of hybrid or arc welding. However, in comparison with the above named methods, laser welding is characterised by very high heating and cooling rates, resulting in diffusionless phase transformations and, consequently, in the obtainment of welded joints characterised by high hardness [11]. The issue of the high hardness of steels from the AHSS group was investigated by Grajcar et al. (using the laser welding of TRIP steels as an example [12]), who stated that the use of new welding techniques (e.g. twin-spot laser welding) improved the quality of welded joints [13]. The use of a twin-spot laser beam reduces the hardness of steels by decreasing the percentage content of martensite in the microstructure [14].

Presently, there are two methods enabling the obtainment of the twin-spot beam, i.e. the use of two lasers or the use of a special optical element making it possible to split a laser beam [15]. Twin-spot laser beam welding is also used for welding galvanised steels, where the first beam is used for creating a duct enabling the discharge of zinc vapours, whereas the second beam is used for making a welded joint as such [16]. Milberg et al. [17] stated that, when welding galvanised steels, the use of the twin-spot beam significantly improves the quality of welded joints (decreases the number of imperfections), in comparison with conventional methods. However, due to an excessively large number of parameters affecting the process of laser welding, the twin-spot laser welding should be thoroughly controlled. Suder et al. [18] reported that, in addition to the power of laser and a welding rate, the quality of a welded joint is also affected by the diameter of a laser beam.

Until today, twin-spot laser welding has not been used for welding Complex Phase high-strength steels. This work discusses the use of various modified welding cycles in order to determine their effects on the microstructure and hardness of joints made of CP steels.

2. Material

In order to determine the effect of twin-spot laser beam power distribution on the microstructure and properties of welded joints made of steel CPW 800, it was necessary to use a 2.5 mm thick steel sheet (150x300 mm). Steel CPW 800 is industrially manufactured hot-rolled steel subjected to controlled cooling. This steel has a fine-grained microstructure composed of a ferritic-bainitic matrix containing martensitic-austenitic (M-A) islands of various sizes and small amounts of retained austenite (γ_R) in the form of fine bright grains (Fig. 1).

* INSTITUTE OF WELDING, 16-18 BL. CZESŁAWA STREET, 44-100 GLIWICE, POLAND

** SILESIAN UNIVERSITY OF TECHNOLOGY, INSTITUTE OF ENGINEERING MATERIALS AND BIOMATERIALS, 18A KONARSKIEGO STR., 44-100 GLIWICE, POLAND

Corresponding author: mateusz.morawiec@polsl.pl

TABLE 1

Chemical composition and carbon equivalent (C_e) of steel CPW 800

C	Mn	Si	Cr	S	P	Nb	Ti	N	Al	Mo	Ce
0.08	1.72	0.56	0.34	0.003	0.010	0.005	0.125	0.002	0.29	0.016	0.46

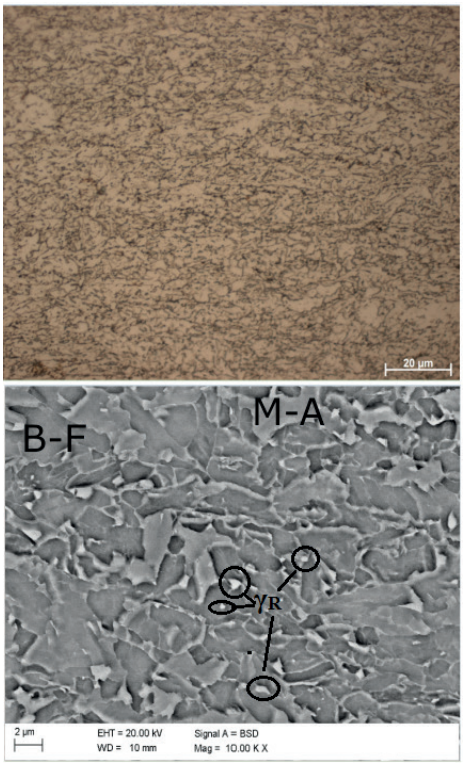

Fig. 1. Microstructure of steel CPW 800 after hot rolling and controlled cooling

The steel subjected to analysis is characterised by a relatively low carbon content (0.08 wt.%) and higher contents of Mn, Si and Cr, increasing the steel hardenability (Table 1). Increased contents of Al and Si prevent carbide precipitation processes [5, 19]. Microadditions of Ti and Nb were added in order to improve the mechanical properties of the steel through the grain refinement and precipitation hardening. On the basis of equation (1), it was possible to calculate the carbon equivalent for the steel subjected to analysis:

$$C_e = C + \frac{Mn}{6} + \frac{Si}{24} + \frac{Ni}{40} + \frac{Cr}{5} + \frac{Mo}{4}\,[\%] \qquad (1)$$

3. Experimental procedure

The welding tests involving the CP steel were performed using the keyhole welding technique, a solid state laser, integrated with a robotic system for laser processing, installed at Instytut Spawalnictwa in Gliwice. The aforesaid laboratory test rig satisfies the requirements of most advanced rigs and is equipped with laser TruDisk 12002 – a Yb:YAG solid-state laser (Trumpf) having a maximum power of 12 kW and laser beam quality designated by the parameter of BPP ≤ 8 mm·mrad and a CFO head (Trumpf) used for single-spot laser welding. The head was connected to the laser source using an optical fibre having a diameter of 200 µm and a focusing lens having a focal length of fog = 300 mm. The diameter of the laser beam focus amounted to 300 µm. The rig was also equipped with a D70 head provided with a system enabling the twin-spot focusing of a laser beam. The distribution of power density between two focuses was monitored using a UFF100 laser beam analyser (Prometec). The tests also involved the selection of an optical fibre and a laser beam focusing lens enabling the obtainment of a laser beam focus having a diameter of 0.6 mm.

In order to ensure the precise positioning of the laser beam along the line of contact, the test sections of the sheets were fixed to the table (constituting an integral part of the rig) using eccentric clamps. The edges of the joint were subjected to square butt weld preparation and fixed without a spacing gap. Welding was performed in air atmosphere.

As regards the D70 head, the twin-spot laser beam is obtained by placing a special optical module across the laser beam, thus changing its trajectory. Afterwards, the beam is focused on two spots by standard focusing lenses. The distance between the focuses of the laser beam is affected by the inclination of the optical module plane. The laser beam power distribution is influenced by the position of the optical module in relation to the laser beam (Fig. 2).

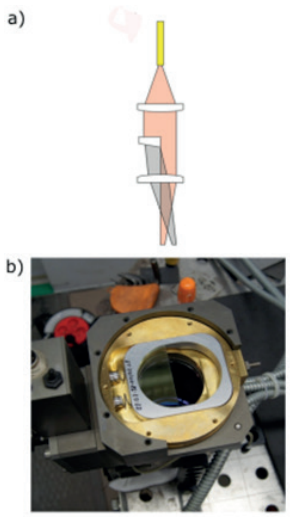

Fig. 2. Manner of obtaining two focuses of the laser beam in solid-state lasers (a) and the exchangeable optical element (b) for splitting the laser beam in the D70 head with the possibility of adjusting laser beam power distribution

The maximum distance between the beam focuses adopted when making the test joints amounted to 4 mm. It was assumed that the tests would be performed with the beam power distribution of 50:50; 60:40 and 70:30 (the first value defines the percentage amount of beam power in the first focusing point of the tandem system). The change in power density distribution consisted in the manual change in the position of the optical module in relation to the laser beam. Each change in the above named position entails a change in density distribution between two focuses and requires

verification. In the tests, the verification of the actual power density distribution was performed using a UFF100 laser beam analyser (Prometec). The graphic representation concerning the results of beam power measurements is shown in Figure 3.

TABLE 2
Parameters of laser welding performed using the beam focused on two spots of the 2.5 mm steel sheet

Specimen no.	101	103	105	107	109	111
Total beam power, kW	6	4	6	4	6	4
Beam power distribution, %	50:50	50:50	60:40	60:40	70:30	70:30
Welding rate, m/min	5.5	2.7	5.5	2.7	5.5	2.7
Linear energy, kJ/mm	0.065	0.090	0.065	0.090	0.065	0.090

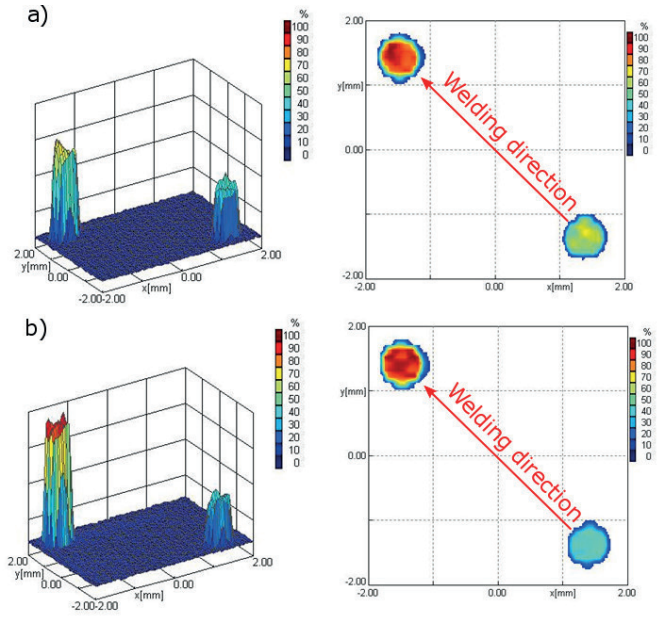

Fig. 3. Graphical representation of laser beam power distribution for: a) distribution of 60:40, b) distribution of 70:30

In order to determine the effect of beam power distribution on the microstructure and properties of the joints made of steel CPW 800, it was necessary to use 6 sets of welding parameters adjusted experimentally in a manner enabling the full penetration of the sheet without compromising the high quality of the joint. The parameters of welding performed using the twin-spot laser beam are presented in Table 2.

The preparation of specimens for macro- and microscopic metallographic tests as well as hardness measurements involved the cutting of the welded joints in the plane perpendicular to the weld axis. The specimens were included in epoxy resin, subjected to grinding by means of abrasive paper and next polished using initially diamond and next corundum slurry. The microstructure of the specimen was revealed by etching in 3% Nital and in the aqueous solution of sodium pyrosulfate. The purpose of the additional etching in sodium pyrosulfate was to reveal grains of retained austenite.

The macro- and microscopic metallographic tests were performed using an MeF4 light microscope manufactured by Leica. Morphological details were revealed using a SUPRA 25 scanning electron microscope in the BSE observation mode, where accelerating voltage amounted to 20 kV. Cross-sectional hardness measurements of the welded joints were performed by means of a KB50BVZ-FA testing machine manufactured by KB Prüftechnik, using an indenter load of 9.81 N (HV1). The tensile tests were performed using an Instron 4210 testing machine.

4. Results and discussion

4.1. Macroscopic observations

In order to assess the effect of linear energy and beam power distribution on the width of the welded joint and on its macrostructure, it was necessary to perform the macroscopic tests of the welded joints. Metallographic images presenting welded joints made using various ratios of laser beam power distribution and various values of linear energy are presented in Figs. 4 and 5. As can be seen, an increase in laser linear energy increased the width of the welded joint. This phenomenon was caused by a greater heat input to the material being welded. The change in the width of the fusion zone and that of the heat affected zone in relation to various values of laser beam power distribution and various values of linear energy is presented in Fig. 6.

Figure 6 reveals that a change in linear energy significantly affects the width of the welded joint. For each beam power distribution ratio, an increase in welding linear energy increased the width of the fusion zone and that of the HAZ. It could also be noticed that the beam distribution itself changed the width of the individual zones. A change in laser beam energy distribution did not significantly affect the width of the heat affected zone. The HAZ width in specimen 101 (Fig. 4a) amounted to 0.5 mm, whereas as regards specimen 105 (Fig. 4b) and 109 (Fig. 4c), the HAZ width amounted to 0.55 mm. Similar observations were made in relation to changes in welding linear energy. It was noticed that the distribution of beam power affected the width of the fusion zone. In specimens welded with a lower linear energy (No. 101, 105 and 109), the fusion zone width amounted to 0.88 mm, 1 mm and 0.94 mm respectively. The decrease in the fusion zone width in specimen 109 was caused by the change in weld geometry resulting from beam power distribution (70%-30%).

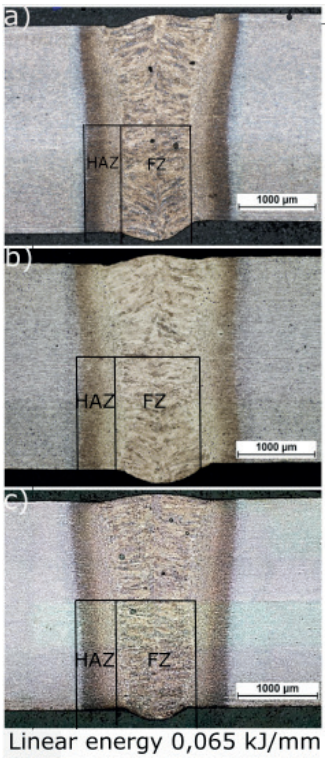

Fig. 4. Macrostructures of the welded joints made of steel CPW 800 in relation to a welding energy of 0.065 kJ/mm and various ratios of beam power distribution: a) 50:50, b) 60:40 and c) 70:30

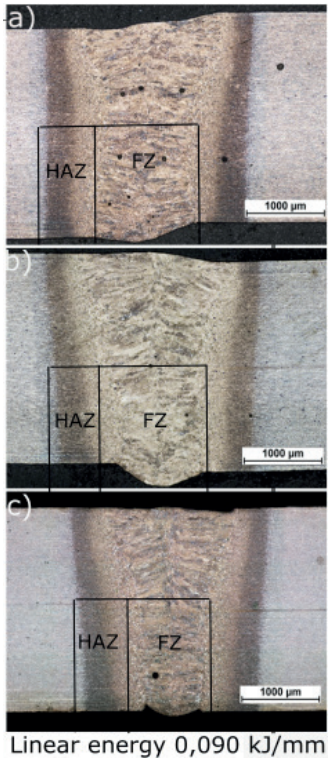

Fig. 5. Macrostructures of the welded joints made of steel CPW 800 in relation to a welding energy of 0.09 kJ/mm and various ratios of beam power distribution: a) 50:50, b) 60:40 and c) 70:30

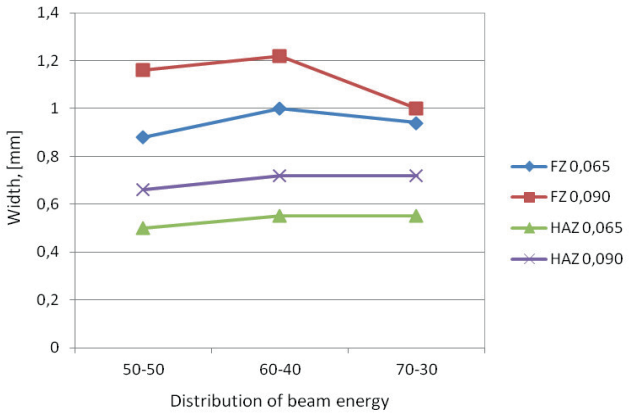

Fig. 6. Curves presenting changes in the width of the fusion zone (FZ) and the width of heat affected zone (HAZ) in relation to various ratios of beam power distribution and various values of welding linear energy

In addition, Figure 6 reveals that a change in beam power distribution affects the geometry of the welded joint, particularly as regards higher linear energy for the power distribution of 60:40 and 70:30. In cases of these beam power distribution ratios, the welded joint was characterised by the greater width of the face than that of the root. The reason for the aforesaid phenomenon was the very low energy of the second beam. Because of the overly low energy, the second beam affected the material only at a certain depth. As a result, the material was subjected to heating on the weld face side, thus increasing the face width. Such an effect can be observed as regards the beam power distribution of 70:30 (specimens 109 and 111) in Figure 6. As can be seen, regardless of linear energy, the width of the central part of the weld is similar in both cases, which demonstrates the insignificant effect of the second beam on the material.

In each case, the macrostructure of the welded joint was composed of columnar crystals oriented in parallel to the direction of heat discharge. In cases of beam power distribution ratios of 60:40 and 70:30, the crystals in the weld face were significantly bigger than those in the root.

4.2. Microscopic Observations

The microscopic tests were performed in order to identify structural constituents in the fusion zone, heat affected zone and in the transition zone between the base material and the heat affected zone. In all the variants subjected to analysis, the microstructure of the fusion zone contained lath martensite (see Figs. 7 and 8). Figures 7 and 8 present the microstructures of the fusion zone for all of the laser welding variants subjected to tests.

Figure 9 presents the morphological details of the fusion zone martensite in relation to twin-spot laser beam welding. Such a microstructure of low-carbon martensite is typical for high-strength dual-phase steels. When the twin-spot laser beam was used, the structure was primarily composed of defragmented martensite containing fine precipitates. Such a martensitic morphology could indicate that a tempering process had taken place (manifested by the presence of precipitates in the microstructure). Xie [10] stated that the use of the twin-spot laser beam decreased the gradient of temperature in the direction perpendicular to the direction of welding and, consequently, reduced the cooling rate of liquid metal. Similar conclusions were drawn by Sokolov et al. [11], who used twin-spot laser beam welding for preheating (the first beam) and welding. Such a process reduces a cooling rate thereby decreasing the hardness of a welded joint. Kuryntsev et al. [20] found that the heating of a welded joint for 2 hours results in the tempering of martensite and improves the quality of a welded joint. In the tests conducted, the time of the second beam exposure was significantly shorter, yet the structural effects visible in Fig. 9 are characterised by features typical of tempered-like microstructures.

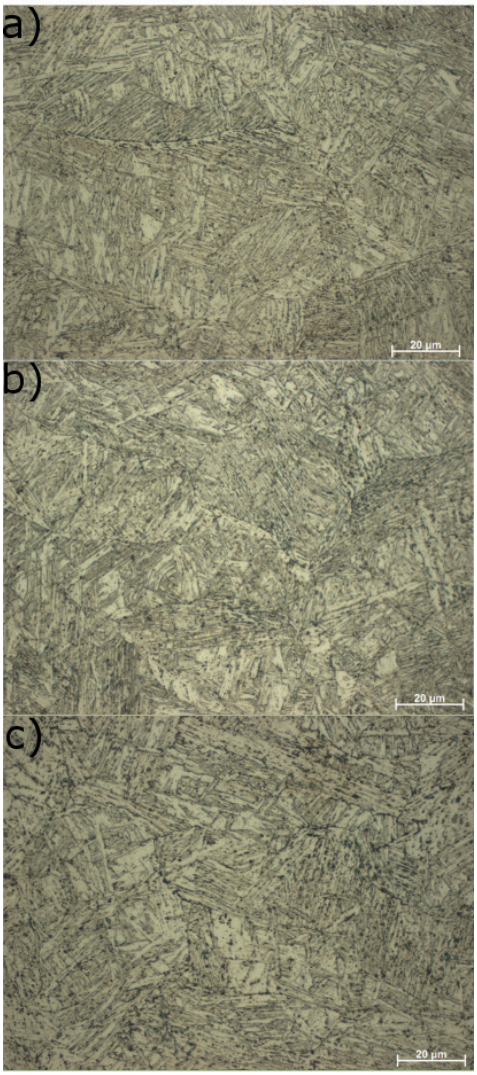

Fig. 7. Microstructure of the fusion zone of steel CPW 800 in relation to various welding methods: a), b), c) welding using a linear energy of 0.065 kJ/mm and the beam power distribution of 50:50, 60:40 and 70:30 respectively

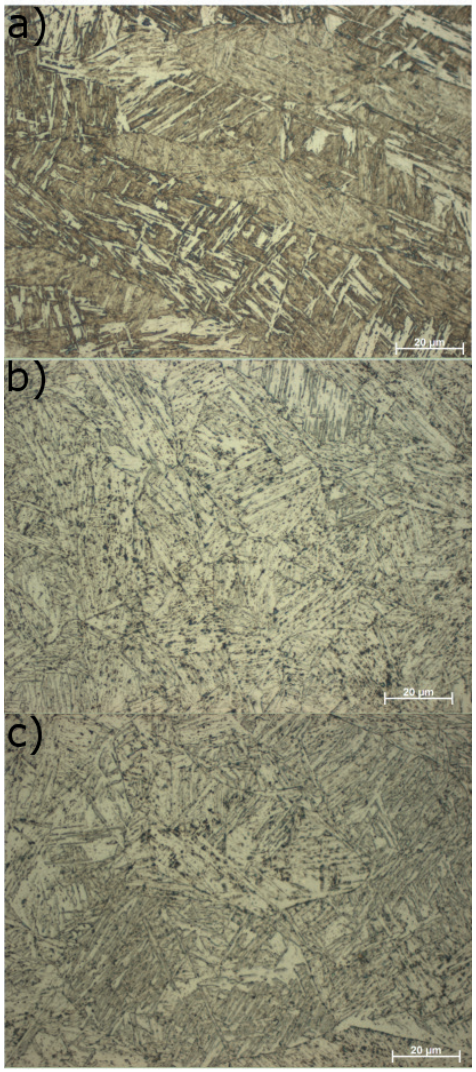

Fig. 8. Microstructure of the fusion zone of steel CPW 800 in relation to various welding methods: a), b), c) welding using a linear energy of 0.09 kJ/mm and the beam power distribution of 50:50, 60:40 and 70:30 respectively

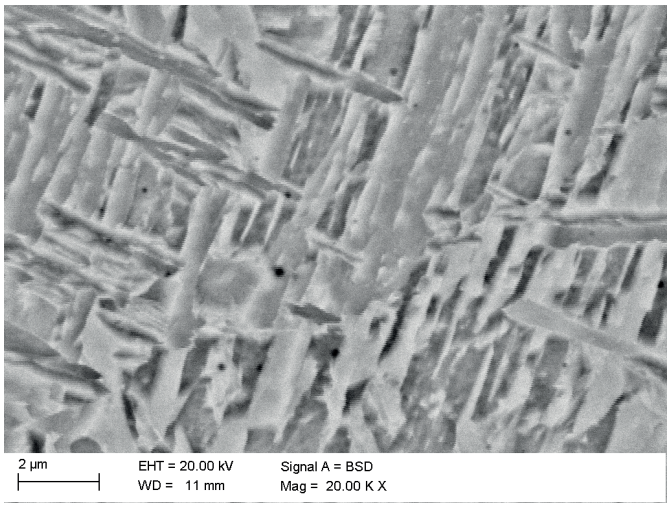

Fig. 9. Detailed microstructure of the fusion zone in steel CPW 800

In all of the cases, the microstructure of the central part of the heat affected zone contained the mixture of bainite and martensite (Fig. 10). The HAZ area close to the fusion line contained lath martensite, whereas the central part of the HAZ contained martensite in the form of blocky grains. The change in beam power distribution did not significantly affect the morphological features of the structure. It was possible to observe the relatively good representation of the prior austenite boundaries (approximately 10 µm in size). The morphology of martensite indicated its partial defragmentation and the presence of fine precipitates, which, in turn, could imply the initiation of tempering processes triggered by the effect of the second beam (Fig. 11). The martensite size is much smaller when compared to the fusion zone.

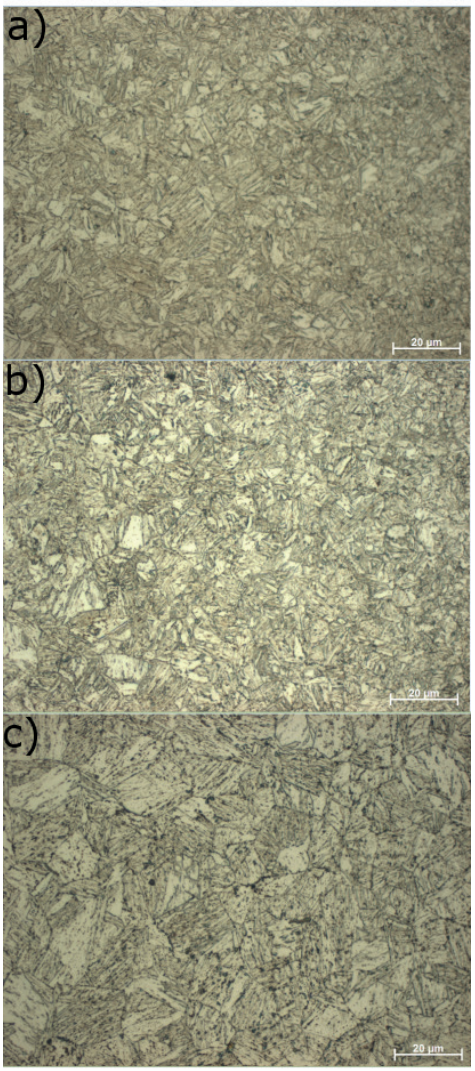

Fig. 10. Representative microstructures of the HAZ relation to a welding energy of 0.065 kJ/mm and various welding methods: a) beam power distribution of 50:50; b) beam power distribution of 60:40 and c) beam power distribution of 70:30

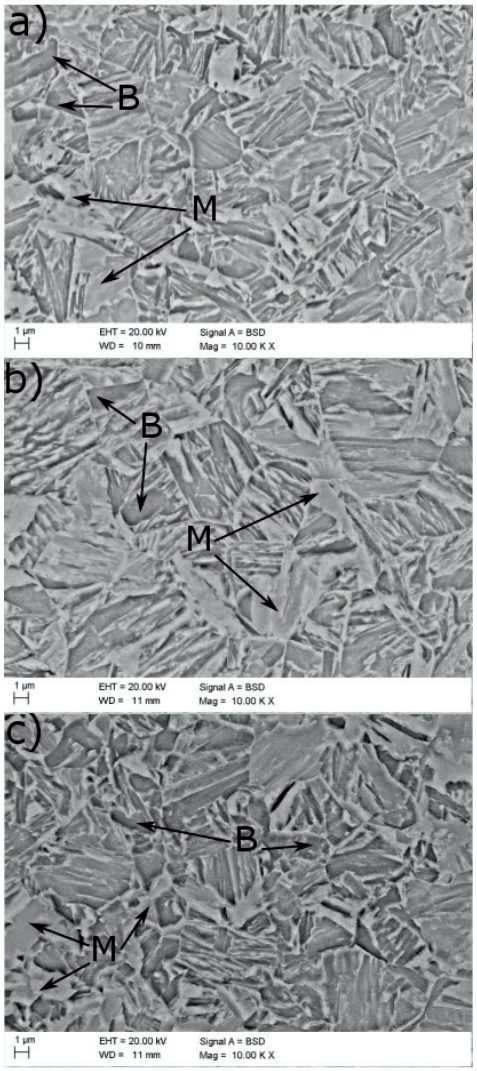

Fig. 11. Representative SEM microstructures of the HAZ relation to a welding energy of 0.065 kJ/mm and various welding methods: a) beam power distribution of 50:50; b) beam power distribution of 60:40 and c) beam power distribution of 70:30

The microstructure of the transition zone between the base material and the HAZ is presented in Figure 12. The microstructure was composed of the fine-grained mixture of ferrite, bainite, martensite and some amount of retained austenite. It was also possible to notice areas of partially transformed austenite, forming MA-type islands (Fig. 13). During cooling, the above named austenite transformed into martensite only in the central part. As a result, austenite was present on the edges of martensitic islands. The content of ferrite increased along with a decreasing distance from the base material and did not depend on the distribution of laser beam power.

Figure 14 presents the detailed microstructure of the transition zone characterised by the presence of fine and bright grains of retained austenite (γ_R). In the microstructure of the transition zone, retained austenite was present in two forms, i.e. as single fine grains or on the edges of martensite blocks. The presence of retained austenite on the edges of martensite grains resulted from the diffusive enrichment of phase γ with carbon during the thermal cycle. Due to the dynamics of the thermal cycle, the only areas enriched with carbon were interphase boundaries α/γ, which during cooling led to the martensitic transformation of the central part of austenite grains (characterised by the lower content of carbon). A similar tendency consisting in the formation of block-like grains of retained austenite in the intercritical range was observed by Grajcar et al. [21] in TRIP steels subjected to thermo-mechanical controlled processing (TMCP). This could imply that, during welding, the temperature of the transition zone was restricted within the intercritical range, favouring the stabilisation of retained austenite.

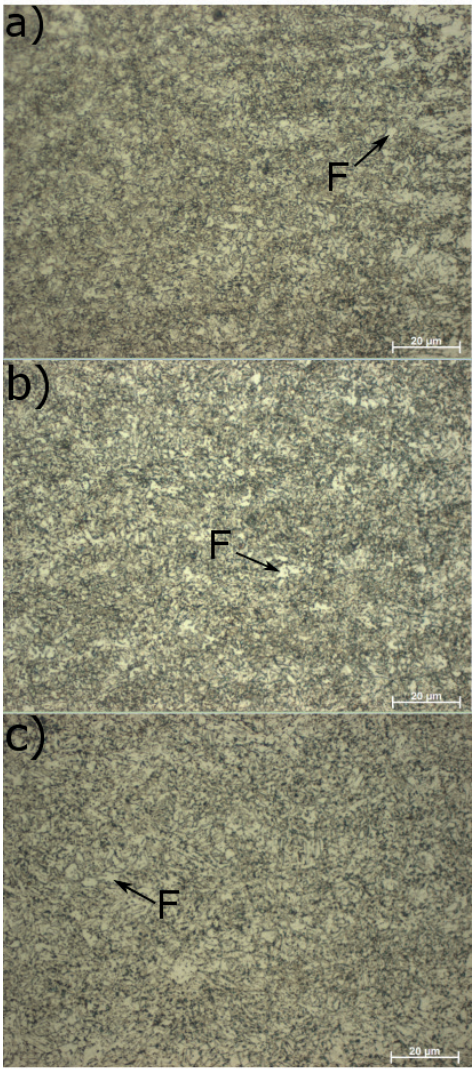

Fig. 12. Selected microstructures of the transition zone in steel CPW 800 in relation to a welding energy of 0.065 kJ/mm and various welding methods: a) beam power distribution of 50:50; b) beam power distribution of 60:40 and c) beam power distribution of 70:30

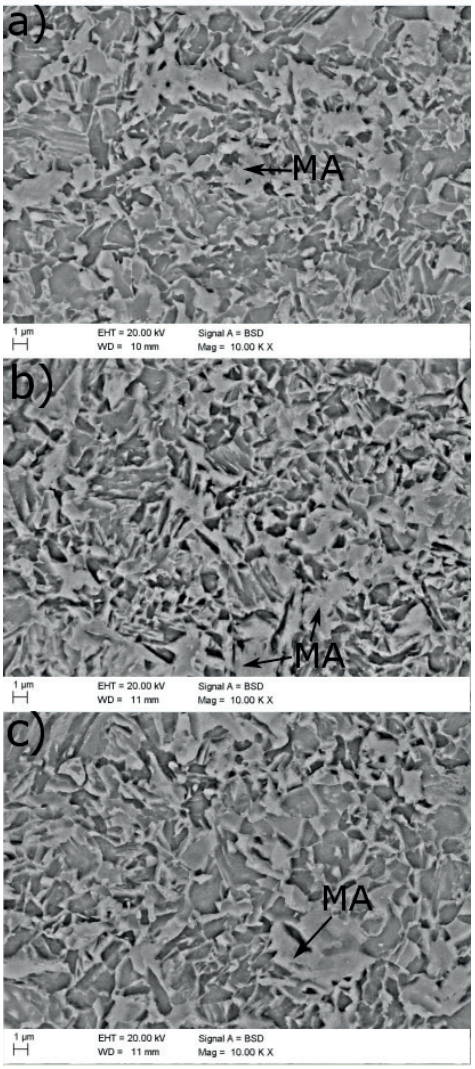

Fig. 13. Representative SEM microstructures of the transition zone in steel CPW 800 in relation to a welding energy of 0.065 kJ/mm and various welding methods: a) beam power distribution of 50:50; b) beam power distribution of 60:40 and c) beam power distribution of 70:30

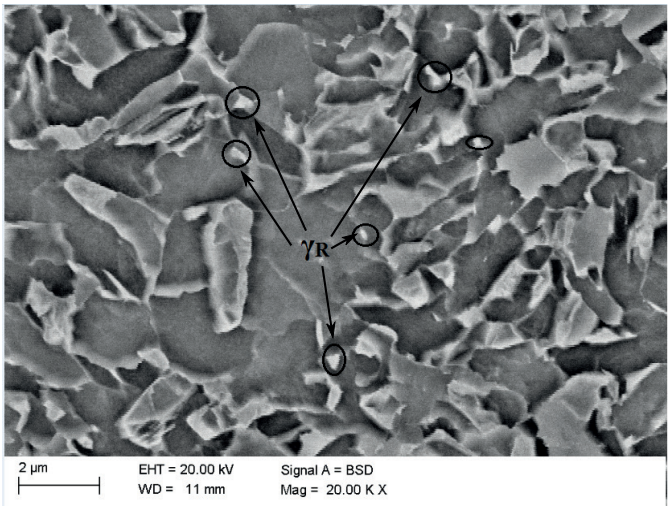

Fig. 14. SEM image showing the microstructure of the intercritical zone containing the large content of retained austenite

4.3. Mechanical properties

In order to determine the quality of the welded joints it was necessary to perform hardness measurements on the cross-section of the weld. The hardness values concerning the cross-section of the weld in relation to each welding variant are presented in Figure 15. The highest hardness amounting to 365 HV1 was found in the welded joint made using a linear energy of 0.065 kJ/mm and the beam power distribution of 50:50. In turn, the lowest hardness of 340 HV1 was measured in the welded joint made using a linear energy of 0.09 kJ/mm and the beam power distribution of 60:40. As can be seen, increasing the linear energy decreased hardness in relation to the same beam power distribution but of lower welding energy. It can also be seen that the power distribution between the first and the second beam affected the hardness of the welded joint.

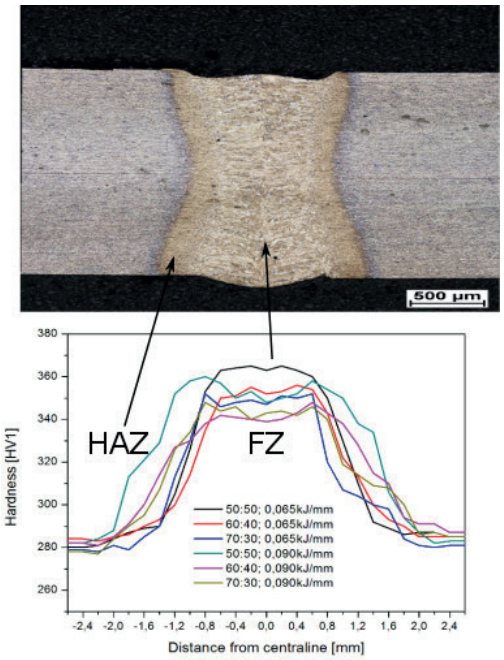

Fig. 15. Results of hardness measurements for all welding variants

Figure 16 presents curves of hardness changes in relation to two values of welding energy and various values of laser beam power distribution. As can be seen, regardless of linear energy, an increase in the energy of the first beam in relation to the second one led to a decrease in hardness; the HAZ was characterised by the highest hardness. The highest hardness was obtained for the beam power distribution of 50:50. An increase in the first beam energy up to 60% reduced hardness significantly. However, a further increase in the energy of the first beam up to 70% was accompanied by only a slight decrease in hardness.

In the case of welding performed using linear energy of 0.065 kJ/mm and the beam power distribution of 70:30, the obtained hardness was by 20 HV1 lower than that obtained for the beam power distribution of 50:50. In the case of a linear energy of 0.09 kJ/mm, the lowest hardness was observed in the welded joint made using the beam power distribution of 60:40 (340 HV1). As regards welding performed using the power distribution of 50:50, where hardness amounted to 350 HV1, a decrease in hardness in the fusion zone was of approximately 10 HV1.

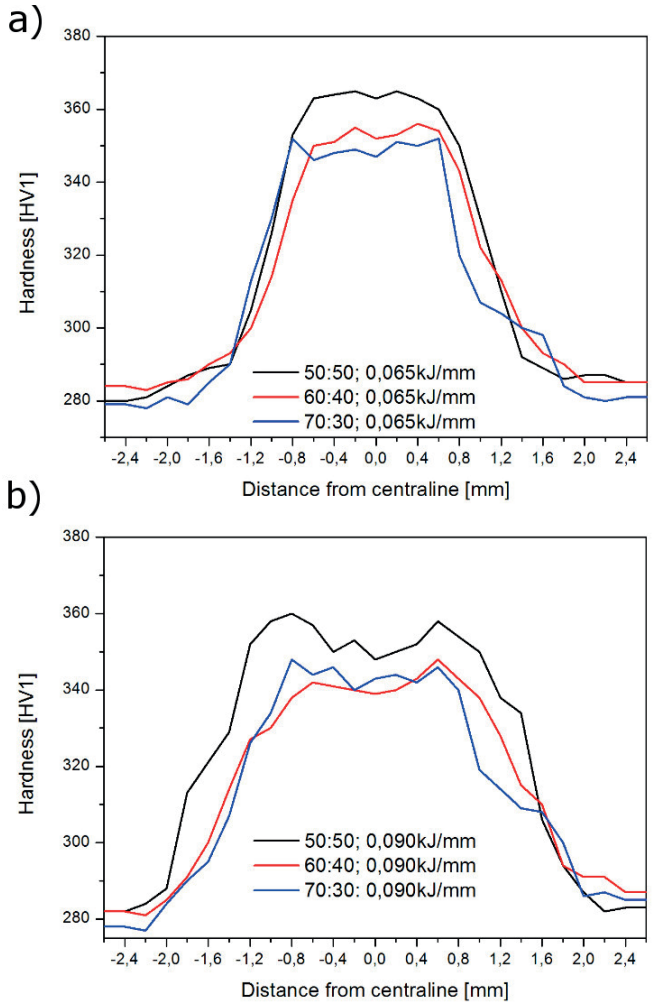

Fig. 16. Effect of beam power distribution on the hardness of the welded joint made using a linear energy of: a) 0.065 kJ/mm and b) 0.09 kJ/mm

The tests of mechanical properties were performed in accordance with PN-EN ISO 4163:2013. For each joint, five tensile tests were performed. The results of the tensile tests involving the joints made using twin-spot laser beam welding are presented in Table 3. The results are characterised by a very small scatter.

TABLE 3

Tensile test results of the welded joints

Variant no.	Tensile strength, UTS [MPa]					Average UTS, [MPa]	Standard deviation, [MPa]
	1	2	3	4	5		
101	858	855	858	858	857	857,5	1,3
103	848	846	845	846	847	846,7	1,2
105	858	859	858	859	859	859,1	0,3
107	865	861	863	863	864	863,7	1,2
109	857	848	855	854	853	853,6	3,0
111	848	847	830	847	846	844,1	6,9
Note: In each case the rupture took place in the base material							

Table 3 reveals that in each case the rupture took place in the base material, which indicates the high quality of the welded joints. It should be noted that the results shown above present the tensile strength of the base material and not of the welded joint.

5. Conclusions

The following conclusions can be drawn from the present study:

- Twin-spot laser beam welding significantly affected the quality of welded joints favourably reducing their hardness in comparison with the hardness of joints made using single-spot laser beam welding.
- The change in beam power distribution affected the geometry of welded joints. Increasing the power of the first beam limited the effect of the second beam on the welded joints. In cases of 60:40 and 70:30 distribution, the weld face was significantly larger than the weld root. The incomplete penetration of the welded joint by the second beams was responsible for significant differences in heat absorbed by the material in its upper and lower part.
- The use of the twin-spot laser beam enabled the obtainment of microstructures having features typical of tempering and characterised by the significant defragmentation of martensitic and bainitic areas. The transition zone contained retained austenite.
- It was ascertained that the hardness of the welded joint depended on the distribution of beam power. An increase in the energy of the first beam up to 60% significantly decreased the hardness of the welded joint; a further increase in the beam energy up to 70% caused an insignificant decrease in hardness. In the case of welding performed using a linear energy of 0.065 kJ/mm, a decrease in hardness amounted to approximately 20 HV1; for a higher linear energy, a decrease in hardness was lower.
- The tensile tests revealed that the welded joint was characterised by tensile strength higher than or equal to that of the base material.

Acknowledgements

The financial support of the Ministry of Science and Higher Education (subvention No. 7430/E-367/M/2016) for young scientists and PhD students is greatfully acknowledged.

REFERENCES

[1] A. Kokosza, J. Pacyna, Mater. Sci. Technol. **31**, (7), 802-807 (2015).
[2] J. Górka, Indian J. Eng. Mater. Sci. 22, (5), 497-502 (2015).
[3] E. Mazancova, P. Wyslych, K. Mazanec, Kovove Mater. **33**, (2), 94-104 (1995).
[4] L.A. Dobrzański, M. Bonek, A. Klimpel, A. Lisiecki, Mater. Sci. Forum **437**, 69-72 (2003).
[5] R. Blonde, E. Jimenez-Melero, L. Zhao, N. Schell, E. Brueck, S. van der Zwaag, N.H. van Dijk, Mater. Sci. Eng. A **594**, 125-134 (2014).
[6] H. Jirkova, L. Kucerova, B. Masek, Mater. Today **2**, (3), 627-630 (2015).
[7] E. Skolek, K. Wasiak, W.A. Świątnicki, Mater. Tehnol. **49**, (6), 933-939 (2015).
[8] M. Jablonska, A. Smiglewicz, Metalurgija **54**, (4), 619-622 (2015).
[9] L.A. Dobrzański, A. Grajcar, W. Borek, Mater. Sci. Forum **638-642**, 3224-3229 (2010).
[10] J. Xie, Weld. J. **81**, 223-230 (2002).
[11] M. Sokolov, A. Salminem, E.I. Khlusova, M.M. Pronin, M. Golubeva, M. Kuznestov, Phys. Procedia **78**, 255-264 (2015).
[12] A. Grajcar, M. Różański, S. Stano, A. Kowalski, J. Mater. Eng. Perform. **23**, (9), 3400-3406 (2014).
[13] A. Grajcar, M. Różański, S. Stano, A. Kowalski, B. Grzegorczyk, Adv. Mater. Sci. Eng. **2014**, article ID 658947, doi.org/10.1155/2014/658947, 8 (2014).
[14] M. Sokolov, A. Salminem, Engineering **6**, 559-571 (2014).
[15] Y. Miyashita, Handbook of laser welding technologies, Woodhead Publishing Limited, Oxford 2013.
[16] S. Igbal, M.M.S. Gualini, F. Grassi, J. Mater. Proc. Tech. **184**, 12-18 (2007).
[17] J. Milberg, A. Trautmann, Prod. Proc. Res. Dev. **3**, (1), 9-15 (2009).
[18] W.J. Suder, S. Williams, Opt. Laser Technol. **56**, 223-229 (2014).
[19] M.S. Weglowski, S. Stano, G. Michta, W. Osuch, Arch. Metall. Mater. **55**, (1), 211-220 (2010).
[20] S.V. Kuryntsev, A.K. Gilimutdinov, Opt. Laser Technol. **74**, 125-131 (2015).
[21] A. Grajcar, K. Radwański, H. Krztoń, Solid State Phenom. **203-204**, 34-37 (2013).